Magnetic Resonance Imaging using Chemical Exchange Saturation Transfer

Jaeseok Park

Department of Brain and Cognitive Engineering, College of Information and Communication, Korea University, Seoul, Republic of Korea

ABSTRACT

Magnetic resonance imaging (MRI) has been widely used as a valuable diagnostic imaging modality that exploits water content and water relaxation properties to provide both structural and functional information with high resolution. Chemical exchange saturation transfer (CEST) in MRI has been recently introduced as a new mechanism of image contrast, wherein exchangeable protons from mobile proteins and peptides are indirectly detected through saturation transfer and are not observable using conventional MRI. It has been demonstrated that CEST MRI can detect important tissue metabolites and byproducts such as glucose, glycogen, and lactate. Additionally, CEST MRI is sensitive to pH or temperature and can calibrate microenvironment dependent on pH or temperature. In this work, we provide an overview on recent trends in CEST MRI, introducing general principles of CEST mechanism, quantitative description of proton transfer process between water pool and exchangeable solute pool in the presence or absence of conventional magnetization transfer effect, and its applications.

Keywords: Magnetic resonance imaging, Chemical exchange saturation transfer, Molecular imaging

1. INTRODUCTION

It was demonstrated in the early 1990s[1–3] that low concentration metabolites could be detected with high sensitivity through the effect of magnetization transfer on the water, which is now known as chemical exchange saturation transfer (CEST) effect. Unlike conventional MRI that exploits water and its relaxation properties to generate high resolution structural and functional information, CEST[1–6] employs the proton exchange process between water and endogenous and exogenous dilute mobile solutes, and has emerged as a novel contrast mechanism that is sensitive to ph- or temperature-dependent microenvironment. In CEST, a frequency selective irradiation pulse is conventionally applied to saturate labile protons in mobile solutes before data acquisition, attenuating the signal intensity of the bulk water due to chemical exchange with the saturated protons. This reduction of signal intensity in the bulk water is typically quantified by the magnetization transfer ratio (MTR), which is defined as the division of the difference of signal intensity between unsaturated and saturated bulk water by the signal intensity of unsaturated one. The indirect measurement of the bulk water signal intensity through magnetization transfer (MT) substantially enhances the detection sensitivity of small solutes that includes exchangeable protons such as NH, OH, and SH groups.[6–11] Additionally, the CEST effects are often pH-dependent. It was demonstrated[2,11,12] that CEST can calibrate a level of pH and is used to detect pH reduction in acute ischema using amide proton transfer (APT).

In this work, we introduce an overview on CEST MRI, dealing with general principles of CEST contrast mechanism, quantitative description of proton transfer process between the water and exchangeable solute pools, and its applications.

Send correspondence to Jaeseok Park (jaeseokpark.biel@gmail.com, Telephone: 82-2-3290-5926)

Nanosystems in Engineering and Medicine, edited by Sang H. Choi, Jin-Ho Choy, Uhn Lee, Vijay K. Varadan,
Proc. of SPIE Vol. 8548, 854846 · © 2012 SPIE · CCC code: 1605-742/12/$18 · doi: 10.1117/12.1000016

2. CEST MECHANISM

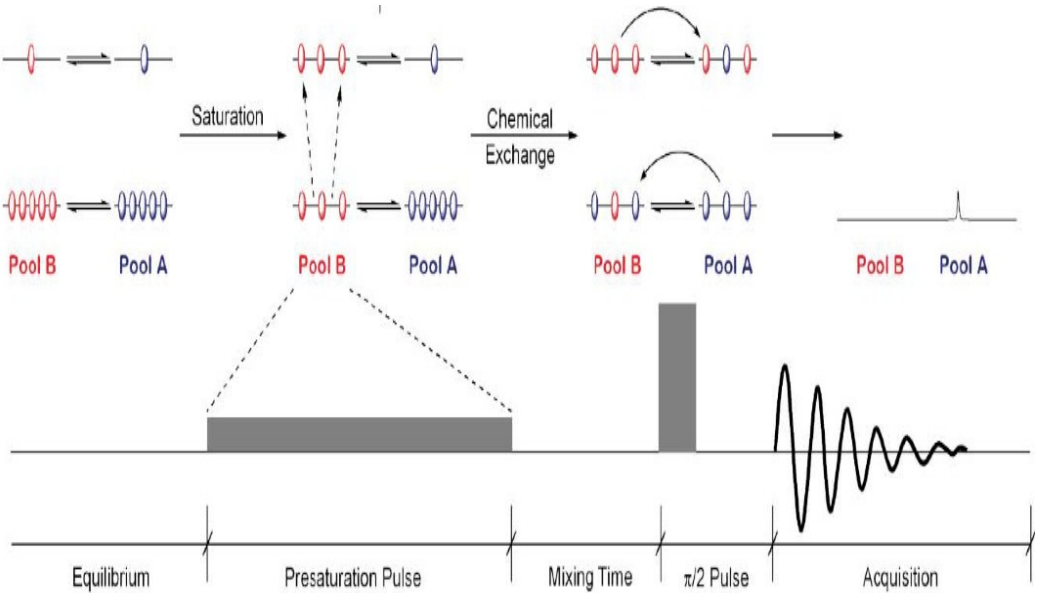

Figure 1. A schematic of CEST mechanism with a two-pool (large water pool A and small solute pool B) model and conventional CEST MR pulse sequence. A radio-frequency pulse saturates solute pool B (energy change from low to high) and chemical exchange attenuates the signal intensity of the bulk water pool A. After a CEST mixing period, imaging data for the bulk water acquired (Woods M. et. al., Chem. Soc. Rev., 2006, 35:500-511[5]).

Figure 1 represents a schematic of CEST mechanism with a two-pool model, wherein a large water pool is represented by pool A while a small solute pool is denoted by pool B, when a radio-frequency (RF) irradiation pulse with low amplitude and long duration is continuously applied. Before applying a pre-saturation RF pulse, concentrations of water and solute protons are in equilibrium. Exchangeable solute protons at a specific resonant frequency are saturated. However, a single chemical transfer of saturation would not be large enough to result in an appreciable signal change in the bulk water.

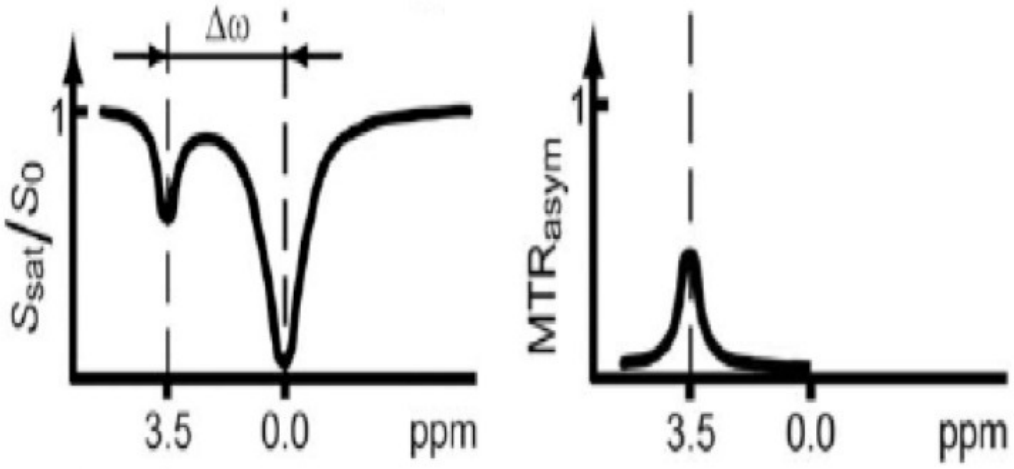

Figure 2. CEST spectrum (left) and MTR_{asym} spectrum (right). During continuous RF irradiation, exchangeable protons in a solute pool are saturated, replaced by unsaturated water protons, and then subsequently saturated again, which attenuates the signal intensity at 3.5ppm (left). MTR shows clear asymmetry at 3.5ppm (right)[13]

Since the water pool is much larger than the solute pool, under the continuous application of the long pre-saturation RF pulse saturated salute protons are replaced by unsaturated water protons, which are subsequently saturated again. Hence, if chemical exchange rate is rapid (millisecond range) and saturation time is sufficiently long (second range), the prolonged RF irradiation yields a substantial effect of saturation, causing sensitivity enhancement to a molar concentration range.

Figure 2 shows CEST spectrum (left) and the asymmetry of MTR spectrum (right). The frequency dependent saturation curve shows the highest saturation effect at 0.0 ppm (water frequency) while exhibiting the symmetric pattern of the direct saturation around the water frequency (spillover effect). On the other hand, CEST effect is visible at the frequency of the low concentration exchangeable solute protons, 3.5 ppm (left). In case the resonant frequency of solute protons is close to the water frequency, spillover effects may interfere with CEST effect. This problem is addressed by employing the $\mathrm{MTR_{asym}}$ spectrum under the assumption that both the spillover and magnetization transfer effects are symmetric around the water frequency (right).

3. QUANTITATIVE DESCRIPTION OF CEST MECHANISM

As is shown in Figure 3, a two-pool proton exchange model is employed: 1) a small solute pool (s) for water-exchangeable protons such as amide protons of mobile proteins and peptides and 2) a large water pool for bulk water protons (w). Assuming that the RF pulse is applied along the x-direction in the rotating frame, the modified Bloch equation, which includes chemical exchange terms (k_{sw}, k_{ws}), is in general written as:

$$\begin{aligned}
\frac{dM_{xs}}{dt} &= -\Delta w_s M_{ys} - R_{2s} M_{xs} - k_{sw} M_{xs} + k_{ws} M_{xw} \\
\frac{dM_{ys}}{dt} &= \Delta w_s M_{xs} + w_1 M_{zs} - R_{2s} M_{ys} - k_{sw} M_{ys} + k_{ws} M_{yw} \\
\frac{dM_{zs}}{dt} &= -w_1 M_{ys} - R_{1s}(M_{zs} - M_{0s}) - k_{sw} M_{zs} + k_{ws} M_{zw} \\
\frac{dM_{xw}}{dt} &= -\Delta w_w M_{yw} - R_{2w} M_{xw} + k_{sw} M_{xs} - k_{ws} M_{xw} \\
\frac{dM_{yw}}{dt} &= \Delta w_w M_{xw} + w_1 M_{zw} - R_{2w} M_{yw} + k_{sw} M_{ys} - k_{ws} M_{yw} \\
\frac{dM_{zw}}{dt} &= -w_1 M_{yw} - R_{1w}(M_{zw} - M_{0w}) + k_{sw} M_{zs} - k_{ws} M_{zw}
\end{aligned} \tag{1}$$

where $M_{xs(w)}$, $M_{ys(w)}$, and $M_{zs(w)}$ are the solute (water) magnetizations in the x, y, and z directions, respectively. NMR parameters are defined as: $w_0 = \gamma B_0$, $w_1 = \gamma B_1$ (where B_0 and B_1 are the main magnetic field strength and the applied RF field strength), and $\Delta w_0 = w - w_0$. It has been known that with raising irradiation power saturation efficiency and spillover effects are increased.[14] Given that saturation efficiency (α) and spillover effects (σ) vary with the RF irradiation power,[14] we simplify Eq. (1) for strong and weak saturation pulse cases, and then extend to general cases with dual two-pool analysis to take into account the inherent symmetry of MTR in in vivo.

3.1 Strong Saturation Pulse

Transverse magnetization perpendicular to the effective z-axis becomes negligible as the RF irradiation power is much stronger than the relaxation and exchange rates. Thus, Eq. (1) is reduced to the

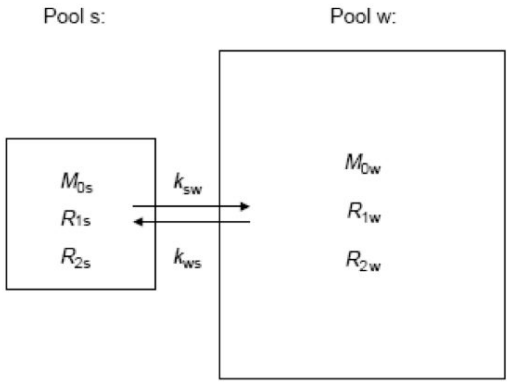

Figure 3. A two-pool exchange model: 1) a small solute pool (s) for exchangeable protons and 2) a large water pool (w) for bulk water protons. $M_{0s(w)}$, $R_{1s(w)}$, and $R_{2s(w)}$ represent concentration of proton, spin-lattice relaxation, and spin-spin relaxation for the solute (water) pool. k_{sw} and k_{ws} are the exchange rates of protons from solute to water, and vice versa.

two equations that describe magnetization components along the effective z-axis. The steady state analytical solution for the bulk water magnetization and spillover factor[14] is shown as:

$$M_{zw} = \frac{R_{1w}R_{zs}cos\theta_w + R_{1s}k_{ws}cos\theta_s cos(\theta_w - \theta_s)}{R_{zw}R_{zs} - k_{ws}k_{sw}cos^2(\theta_w - \theta_s)} M_{0w} \tag{2}$$

$$\sigma = 1 - \frac{r_{1w}}{k_{ws}} \left(\frac{R_{1w}r_{2s}cos^2\theta + R_{1s}k_{ws}cos\theta cos^2(\theta/2)}{r_{zw}r_{zs} - k_{ws}k_{sw}cos^2(\theta/2)} - \frac{R_{1w}r_{2s}cos^2\theta}{r_{zw}r_{2s} - k_{ws}k_{sw}sin^2\theta} \right) \tag{3}$$

where $\theta_{w(s)} = tan^{-1}\left(\frac{w_1}{\Delta w_{w(s)}}\right)$, $r_{1w(s)} = R_{1w(s)} + k_{sw(sw)}$, $r_{2w(s)} = R_{2w(s)} + k_{sw(sw)}$, and $r_{zw(s)} = r_{1w(s)}cos^2\theta_{w(s)} + r_{2w(s)}sin^2\theta_{w(s)}$

As magnetization transfer effects are typically quantified using MTR, the proton transfer rate (PTR) in CEST for the strong saturation pulse is defined as:

$$PTR_{strong} = \frac{M_{0w} - M_{zw}}{M_{0w}} = \frac{k_{ws}}{r_{1w}}(1 - \sigma) \tag{4}$$

3.2 Weak Saturation Pulse

Assuming that only solute protons are saturated using a weak saturation pulse and thus spillover effects are negligible, Δw_s and Δw_w in Eq. (1) approach 0 and ∞, respectively. Thus, Eq. (1) is reduced to the following four equations:

$$\begin{aligned}
\frac{dM_{ys}}{dt} &= w_1 M_{zs} - R_{2s}M_{ys} - k_{sw}M_{ys} + k_{ws}M_{yw} \\
\frac{dM_{zs}}{dt} &= -w_1 M_{ys} - R_{1s}(M_{zs} - M_{0s}) - k_{sw}M_{zs} + k_{ws}M_{zw} \\
\frac{dM_{yw}}{dt} &= -R_{2w}M_{yw} + k_{sw}M_{ys} - k_{ws}M_{yw} \\
\frac{dM_{zw}}{dt} &= -R_{1w}(M_{zw} - M_{0w}) + k_{sw}M_{zs} - k_{ws}M_{zw}
\end{aligned} \tag{5}$$

Given that the left hand side of Eq. (4) is zero, the steady state analytical solution is expressed as:

$$\begin{aligned} M_{zs} &= M_{0s} - \frac{w_1^2 M_{0s}}{w_1^2 + pq}, & M_{ys} &= -\frac{w_1 q M_{0s}}{w_1^2 + pq} \\ M_{zw} &= M_{0w} - \frac{k_{sw}}{r_{1w}} \frac{w_1^2 M_{0s}}{w_1^2 + pq}, & M_{yw} &= -\frac{k_{sw}}{r_{2w}} \frac{w_1 q M_{0s}}{w_1^2 + pq} \end{aligned} \tag{6}$$

where $p = r_{2s} - \frac{k_{sw} k_{ws}}{r_{2w}}$, $q = r_{1s} - \frac{k_{sw} k_{ws}}{r_{1w}}$. Saturation efficiency (α) can be found in Eq. (6) as $\alpha = \frac{w_1^2}{pq + w_1^2}$.

Hence, the PTR for the weak saturation pulse is defined as:

$$PTR_{weak} = \frac{k_{ws}}{r_{1w}} \alpha = \frac{k_{ws}}{r1w} \frac{w_1^2}{pq + w_1^2} \tag{7}$$

3.3 General Analysis

To accommodate saturation efficiency and spillover effects over a full range of the irradiation RF powers, the PTRs of the two extreme saturation cases can be generalized by normalizing the product of Eqs. (4) and (7) by the maximal PTR:

$$PTR = PTR_{weak}(1 - \sigma) = \frac{k_{ws}}{r_{1w}} \alpha (1 - \sigma) \tag{8}$$

Eq. (8) represents implicitly that PTR increases with RF power due to enhanced saturation efficiency while it decreases with further increase of RF power due to rising spillover effects.

Although the two-pool model has been useful in describing CEST in solution, it may not be valid in vivo due to conventional MT effect that includes the inherent asymmetry (MTR'_{asym}) of MTR:[15]

$$MTR_{asym} = MTR'_{asym} + PTR \tag{9}$$

To eliminate conventional MT effect that contains MTR'_{asym}, a dual two-pool model was suggested for amide proton transfer rate (APTR) during acute ischemia[12] using the APTR contrast between contralateral(c) and ipsilateral(i) hemispheres as:

$$\Delta APTR = MTR^c_{asym} - MTR^i_{asym} = APTR^c_{weak}(1 - \sigma^c) - APTR^i_{weak}(1 - \sigma^i) \tag{10}$$

The APTR contrast with the dual two-pool model provides simplified quantification of CEST in vivo independent of conventional MT effects.

4. CONCLUSION

We introduced an overview on basic principles and quantitative analysis of CEST. The endogenous and exogenous contrast agent in CEST provides potentially novel image contrast, which includes pH imaging, metabolite detection, metal ion detection, liposome labeling, nano particle labeling, and imaging of OH groups, etc. The CEST principle can be exploited to design exogenous multi-functional contrast agents ranging from powerful paramagnetic agent to simple biodegradable peptides and sugars, which truly extends the utility of conventional MRI to molecular imaging fields.

5. ACKNOWLEDGMENTS

This research was supported by Mid-Career Researcher Program (2011-0016116), and World Class University Program (R31-10008) through the National Research Foundation of Korea (NRF) grant funded by the Ministry of Education, Science and Technology (MEST).

REFERENCES

[1] Wolff, S. D. and Balaban, R. S., "Magnetization transfer contrast (mtc) and tissue water proton relaxation in vivo," *Magn Reson Med* **10**, 135–144 (Apr 1989).

[2] Ward, K. M. and Balaban, R. S., "Determination of ph using water protons and chemical exchange dependent saturation transfer (cest)," *Magn Reson Med* **44**, 799–802 (Nov 2000).

[3] Guivel-Scharen, V., Sinnwell, T., Wolff, S. D., and Balaban, R. S., "Detection of proton chemical exchange between metabolites and water in biological tissues," *J Magn Reson* **133**, 36–45 (Jul 1998).

[4] Zhou, J., Blakeley, J. O., Hua, J., Kim, M., Laterra, J., Pomper, M. G., and van Zijl, P. C., "Practical data acquisition method for human brain tumor amide proton transfer (apt) imaging," *Magn Reson Med* **60**, 842–849 (Oct 2008).

[5] Woods, M., Woessner, D. E., and Sherry, A. D., "Paramagnetic lanthanide complexes as paracest agents for medical imaging," *Chem Soc Rev* **35**, 500–511 (Jun 2006).

[6] van Zijl, P. C., Jones, C. K., Ren, J., Malloy, C. R., and Sherry, A. D., "Mri detection of glycogen in vivo by using chemical exchange saturation transfer imaging (glycocest)," *Proc Natl Acad Sci U S A* **104**, 4359–4364 (Mar 2007).

[7] Ward, K. M., Aletras, A. H., and Balaban, R. S., "A new class of contrast agents for mri based on proton chemical exchange dependent saturation transfer (cest)," *J Magn Reson* **143**, 79–87 (Mar 2000).

[8] Woessner, D. E., Zhang, S., Merritt, M. E., and Sherry, A. D., "Numerical solution of the bloch equations provides insights into the optimum design of paracest agents for mri," *Magn Reson Med* **53**, 790–799 (Apr 2005).

[9] Zhang, S., Merritt, M., Woessner, D. E., Lenkinski, R. E., and Sherry, A. D., "Paracest agents: modulating mri contrast via water proton exchange," *Acc Chem Res* **36**, 783–790 (Oct 2003).

[10] Aime, S., Barge, A., Delli Castelli, D., Fedeli, F., Mortillaro, A., Nielsen, F. U., and Terreno, E., "Paramagnetic lanthanide(iii) complexes as ph-sensitive chemical exchange saturation transfer (cest) contrast agents for mri applications," *Magn Reson Med* **47**, 639–648 (Apr 2002).

[11] Zhou, J., Payen, J. F., Wilson, D. A., Traystman, R. J., and van Zijl, P. C., "Using the amide proton signals of intracellular proteins and peptides to detect ph effects in mri," *Nat Med* **9**, 1085–1090 (Aug 2003).

[12] Sun, P. Z., Zhou, J., Huang, J., and van Zijl, P., "Simplified quantitative description of amide proton transfer (apt) imaging during acute ischemia," *Magn Reson Med* **57**, 405–410 (Feb 2007).

[13] van Zijl, P. C. and Yadav, N. N., "Chemical exchange saturation transfer (cest): what is in a name and what isn't?," *Magn Reson Med* **65**, 927–948 (Apr 2011).

[14] Sun, P. Z., van Zijl, P. C., and Zhou, J., "Optimization of the irradiation power in chemical exchange dependent saturation transfer experiments," *J Magn Reson* **175**, 193–200 (Aug 2005).

[15] Hua, J., Jones, C., Blakeley, J., Smith, S., van Zijl, P., and Zhou, J., "Quantitative description of the asymmetry in magnetization transfer effects around the water resonance in the human brain," *Magnetic Resonance in Medicine* **58**(4), 786–793 (2007).